

# Molecular Hydrogen Tracking In An Electrolytic Polishing Process

L.M.A. Ferreira, CERN, Geneva, Switzerland  
CERN, CH-1211 Geneva 23, leonel.ferreira@cern.ch

**Abstract:** In a water based electrolytic polishing process, the formation of molecular hydrogen at the cathode is unavoidable and it can contribute to the formation of surface defects at the anode side. This paper presents the work to model and simulate the molecular hydrogen flow inside radio frequency cavity geometries and compares it with the presence, type and relative position of certain defects in real radio frequency components that went through an electrolytic polishing process. Geometry and flow optimisation hints to reduce molecular hydrogen induced surface defects are also presented.

**Keywords:** Electrolytic polishing, bubbly flow.

## 1. Introduction

In an electrolytic polishing process, the metal part to be polished is made anodic and, within a certain range of working parameters, it undergoes a controlled oxidation/etching reaction that allows a polished finishing. Depending on the electrolyte and of the metal, the metal dissolution (anodic reaction) can have a yield of 100% and thus no molecular oxygen is formed at the metal surface; this is the case in the present study. On the other hand, the main cathodic reaction is the reduction of hydrogen from the acidic solution into molecular hydrogen ( $H_2$ ).

Previous work [1], [2] done on the optimisation of the electrolytic polishing process didn't directly take into account the impact of the molecular hydrogen formed at the cathode. Although, it isn't expected to change dramatically the fluid dynamics, molecular hydrogen can be source of undesirable local effects. As mentioned in [3],  $H_2$  modifies solution mixing, obstructs electric current flow and also disrupts the viscous layer necessary to achieve a well-polished surface.

The results achieved during previous works have clearly indicated that  $H_2$  was the main responsible for some surface defects (pinholes and grooves) that were observed after electrolytic polishing of niobium on a vertical stand; some of these defects are illustrated in figure 1. The same

conclusion was reached independently by several laboratories [4].

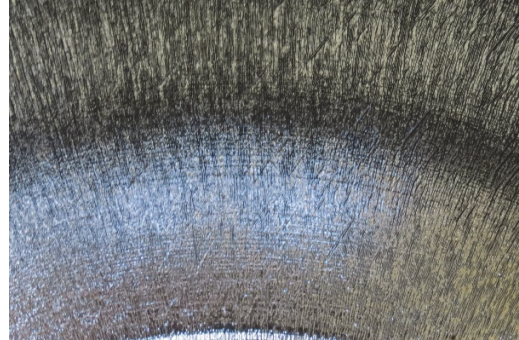


Figure 1: Defects on a polished surface. Pinholes and radial grooves.

Therefore the production and role of  $H_2$  become now one of the most important parameters to be tackled, as the remaining defects are mainly related with hydrogen bubbles. In particular, it becomes important to simulate how  $H_2$  evolves inside the electrochemical cell with different working parameters and cathode geometries.

## 2. Input data and assumptions

Besides the geometry of a mono cell cathode, working parameters like molecular hydrogen bubbles size, bath flow and  $H_2$  mass flow were taken as variables for the different simulations.

Two existing cathode geometries were taken as inputs for the simulation (Figure 2); both geometries are axisymmetric. One geometry, hereafter referred as old cathode, was defined taking into account only the current density distribution optimisation within the electrochemical physics. Further work, integrating fluid dynamics physics, gave origin to a second cathode geometry, hereafter referred as new cathode. For both geometries, the flow inlet is defined by the bottom horizontal plane and the outlet by the top horizontal plane. For the old cathode, the geometry is defined by the vertical polynomial line on the left side close to  $r = 0$  (Figure 2, left), where the active part is the arc line between the two bumps. For the new cathode, the geometry is defined by the sequence of rectangles

on the left side, at  $r = 28$  mm (Figure 2, right), where all surfaces are active. The anode or the surface to be processed (polished) is defined by the vertical polynomial line on the right side (Figure 2, left and right) representing a mono cell cavity geometry.

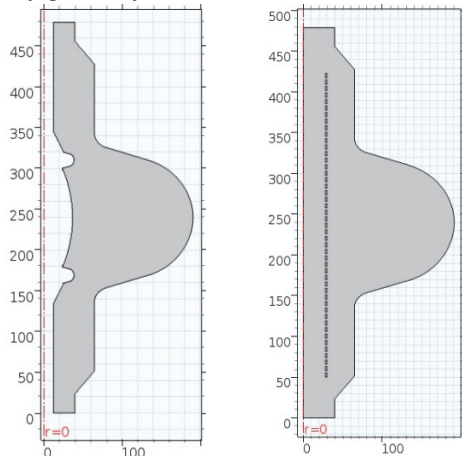


Figure 2: Old cathode (left) and new cathode (right) axisymmetric geometry representation. Axis values are in mm.

The hydrogen bubble diameter was the most difficult variable to evaluate. Experimental observation pointed to a sub millimetre size at the cathode detachment point. As mentioned in [3], many parameters affect this size and therefore a range from a minimum (0.03 mm) to a maximum (1 mm) diameter was considered in the simulation. This includes the full range found in literature [5], 0.03 to 0.5 mm in diameter. It was assumed that the hydrogen bubbles wouldn't evolve in size during their lifetime inside the electrochemical cell. It's an experimental evidence that many coalesce, namely in presence of an obstacle; however, it's not evident that this happens when travelling in the free electrolyte. In fact, in a beaker with sufficient agitation, the electrolyte evolves with time to a macroscopic homogenous two phase solution with no significant sign of coalescence of hydrogen bubbles.

Bath flow impact was checked within the experimental working range i.e., from 5 to 20 litres per minute.

The  $H_2$  mass flow is given by the total applied current on the electrochemical cell; the simulated values where within the minimum and maximum values taken from experimental data,  $2.3 \times 10^{-7}$  to  $5 \times 10^{-7}$   $kg \cdot s^{-1}$ . The  $H_2$  source on the

electrochemical cell is placed at the cathode active surface, where hydrogen is reduced to its molecular form; molecular hydrogen is a gas at the working pressure and temperature. It was assumed that  $H_2$  mass flow would be distributed uniformly along the cathode surface and that all applied current, on the cathode side, was consumed to form  $H_2$ .

Although, the input values are discrete, one underlying objective was to identify if there was a threshold value within the different variables that would lead to a different result in terms of gas phase distribution at the anode wall.

### 3. Use of COMSOL Multiphysics® Software

The model presented here used the Turbulent Bubbly Flow physics module and followed some suggestions found on the airlift loop reactor application (Application ID: 10356) [7], namely the use of a Heaviside function to smooth the initial value of the molecular hydrogen and bath flow.

The study was done as time dependent in order to evaluate the time needed to reach a stationary regime in comparison with the process duration.

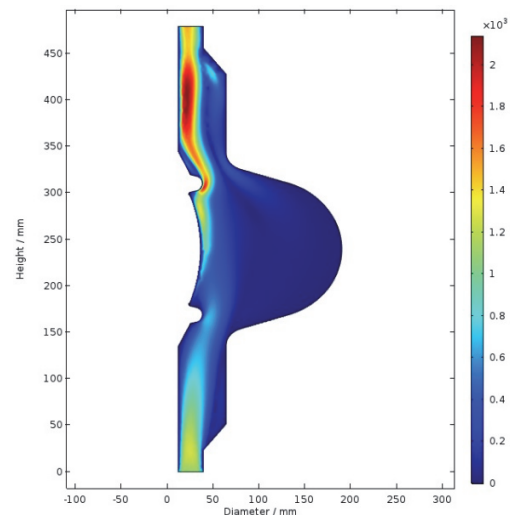


Figure 3: Reynolds number distribution in the electrochemical cell with the old cathode geometry.

The most important choice to define the model was between Laminar and Turbulent modules. The turbulent module was the chosen one as it provided data in agreement with

experimental observations; and this albeit some contradictory data as exposed hereafter.

Figure 3 shows an axisymmetric representation of the Reynold number distribution in the tested electrochemical cell with the old cathode geometry. The obtained values would suggest the use of the laminar module as it is possible to see in figure 3, where locally the Reynolds number barely overcomes 2100 threshold value for turbulent flow.

Figure 4 shows the molecular hydrogen phase volume fraction distribution with the laminar (left) and the turbulent (right) modules for the same input parameters. The white area inside the electrochemical cell represents the volume where the molecular hydrogen phase is absent. The laminar module suggests that hydrogen bubbles would simple move upwards; however, these results aren't consistent with experimental observation, where hydrogen bubbles, once detached from the cathode, flow easily away guided by minor flow patterns. On the other hand, the turbulent module suggest that they also move sideways and more, that they are prone to accumulate on certain regions of the anode surface; in fact, exactly the regions that have shown the highest concentration of defects.

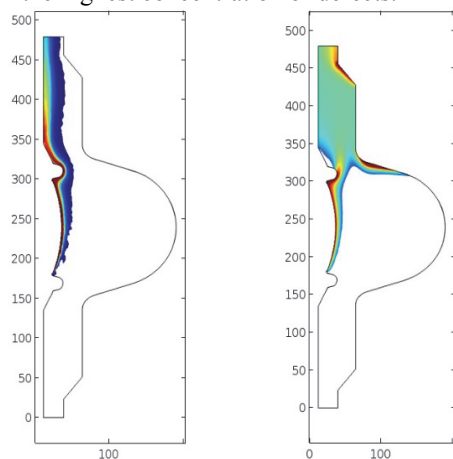


Figure 4: H<sub>2</sub> volume fraction distribution simulated with the laminar module (left) and turbulent module (right) on the old cathode geometry.

The choice between the two modules won't be further elaborated, but complexity of the geometry and the added flow dynamics accounted for the hydrogen bubbles might explain why the Laminar Bubbly Flow module was unable to reproduce experimental observations.

## 4. Results and discussion

Hereafter, the impact of the different variables is presented. The results for the old cathode will only be presented to compare with the new cathode; the influence of all remaining variables on the hydrogen bubble distribution will only be presented for the new cathode geometry. The results from the time resolved study won't be presented here, but the outcome is that after a few minutes, the electrochemical cell was able to reach stationary conditions; this duration is negligible if compared with the process running time that counts for several hours.

### 4.1 New versus Old cathode

Although, a specific study like the present one wasn't made at that time, experimental tests gave enough confidence that the second geometry would behave better in terms of hydrogen bubbles induced defects.

In figure 5, the H<sub>2</sub> phase distribution inside the electrochemical cells with the two different cathodes and the impact of two different bubbles size is represented. The different lines, besides the black line, that represent the anode wall geometry, represent the H<sub>2</sub> phase volume fraction in contact with the anode wall. It clearly shows a reduction of the gas phase fraction in contact with the wall in the case of the new cathode geometry; however locally the values remain high and can go up to 4%.

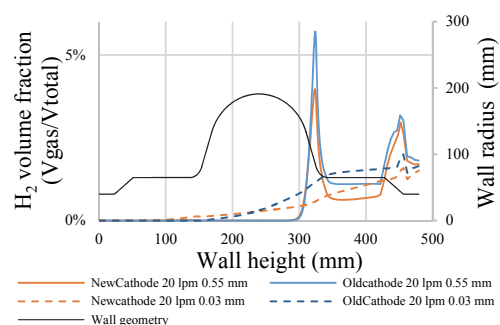


Figure 5: H<sub>2</sub> phase distribution on the electrochemical cell wall.

### 4.2 Hydrogen bubble size

As mentioned before, the hydrogen bubbles size was the most laborious variable to be defined and modelled. The simulation results corroborate the sensitivity to this variable as even with the simplifying assumptions and reduced working

range (below 1 mm diameter), it was possible to identify one threshold value in terms of hydrogen volume fraction distribution in function of bubble size.

Thus, from the simulation results it is possible to separate two trends. In figure 6 is presented the H<sub>2</sub> volume fraction distribution for the two different trends, as well as for the threshold value. The colour scale of figure 6 is limited at 2% volume fraction to enhance the H<sub>2</sub> distribution difference.

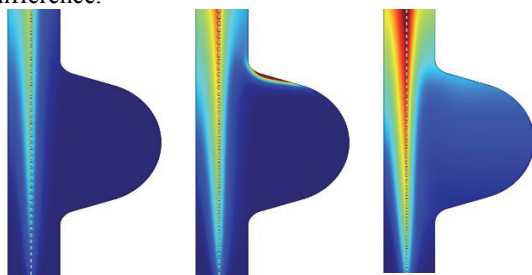


Figure 6: H<sub>2</sub> volume fraction distribution for different hydrogen bubble sizes: 1 mm (left); 0.55 mm (centre) and 0.1 mm (right).

The first trend is observed for hydrogen bubbles sizes above 0.55 mm in diameter; as the hydrogen bubbles size increases, their accumulation on certain wall segments decreases and there are less bubbles in solution, since they are prone to flow directly upwards. The second trend is observed for bubble sizes below 0.55 mm; as hydrogen bubble size decreases, their accumulation on certain wall segments decreases and more bubbles are present in the bulk solution. This second trend becomes dominant for bubbles sizes below 0.1 mm in diameter.

At the threshold value for the hydrogen bubble size, identified at 0.55 mm in diameter, the simulation displays high values of H<sub>2</sub> volume fraction accumulation at certain wall segments. This occurs in the intermediate range of bubble diameter values, going from 0.25 to 0.85 mm and this corresponds to a predominant accumulation behaviour.

It's fundamental to understand how these different behaviours impact on the relative concentration of the H<sub>2</sub> at the anode wall, as only at this location H<sub>2</sub> is able to affect the polishing process and resulting defects. Thus, in figure 7 is a representation of the H<sub>2</sub> volume fraction at the anode wall for the three situations as defined in figure 6. As hydrogen bubbles size decreases, the H<sub>2</sub> concentration increases at specific wall segments until the bubble size threshold value is

reached; at this stage, the rise in concentration is only true on certain wall segments where bubbles upwards flow is hindered by less favourable wall

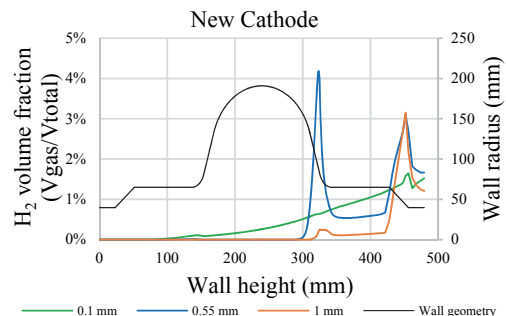


Figure 7: H<sub>2</sub> volume fraction at the anode wall in function of the hydrogen bubble diameter.

slope angles; these wall segments are well identified in figure 7 by peaks of the H<sub>2</sub> volume fraction. After the threshold value, the peaks decrease at the same time as the concentration away from the wall increases; this stage becomes dominant for bubbles sizes below 0.1 mm in diameter. The concentration at the wall becomes a representation of the H<sub>2</sub> fraction of the nearby bulk electrolyte concentration.

#### 4.3 Bath flow

Figure 8 puts into evidence the impact of the bath flow on the H<sub>2</sub> volume fraction at the anode wall. It's clear that as the flow increases, the concentration of the hydrogen bubbles at the wall, decreases; this suggest a flushing effect from the liquid phase on the H<sub>2</sub>. This effect remains independently of the other working parameters, only the H<sub>2</sub> concentration and profile changes.

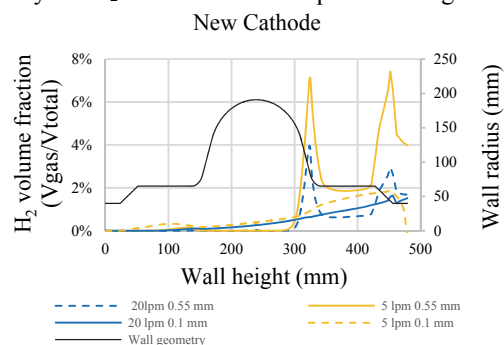


Figure 8: H<sub>2</sub> volume fraction at the anode wall in function of the flow for two hydrogen bubble sizes.

#### 4.4 Hydrogen mass flow

In figure 9, is represented the hydrogen volume fraction at the anode wall in function of

the molecular hydrogen mass flow. Within the studied range, the concentration of hydrogen at the wall increases with increasing hydrogen mass flow.

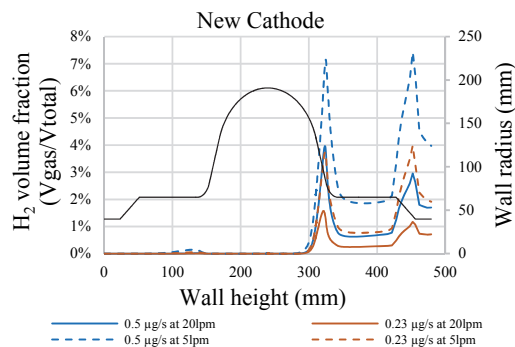


Figure 9: H<sub>2</sub> volume fraction at the anode wall in function of the hydrogen mass flow and for bath flows.

## 5. Conclusions

The present work allowed to understand how H<sub>2</sub> bubbles behave as a function of working parameters and to quantify their distribution inside a defined electrochemical cell geometry.

In terms of cathode geometry it was possible to confirm the improvement made from the old cathode to the new cathode with respect to hydrogen bubble flow; however, this improvement is not as marked as originally thought.

From this study the hydrogen bubbles size results to be the most important variable. Above 1 mm in diameter, bubbles are prone to move mainly upwards, while below 0.1 mm they are prone to move also horizontally, without sticking to the anode wall. This leaves an intermediate range of bubbles diameter where they are prone to accumulate on wall segments that hinder their upward movement.

The bath flow impact was in line with expectations. Although high flow values can reduce the fraction of H<sub>2</sub> bubbles at the anode wall, it's an experimental evidence that it's also responsible for the creation of groove-like defects.

As for bath flow, hydrogen mass flow was in line with expectations. Higher mass flows imply higher H<sub>2</sub> bubbles concentration at the anode wall. Previous work already optimised this parameter by reducing the total applied current to a minimum.

This work gives the orientation for future optimisation paths. It's fundamental to measure precisely the real size of the H<sub>2</sub> bubbles as their behaviour depends on it and this for a relatively narrow range. A membrane might be a solution to trap bubbles avoiding that they reach the anode wall. The cathode geometry can be further optimised by moving the active cathode surface to a more axial position, well apart from the anode.

## 9. References

1. L. M. A. Ferreira et al., "Niobium cavity electropolishing modelling and optimisation", SRF2013, Paris, France (2013)
2. L. M. A. Ferreira et al., "Electropolishing simulation on full scale radio frequency elliptical structures", LINAC14, Geneva, Switzerland (2014)
3. C.A.C. Sequeira et al., Physics of electrolytic gas evolution, Braz. Journal of Physics, **Volume 43**, 199-208 (2013)
4. F. Eozenou et al., "Development of vertical electropolishing process applied on 1300 and 704 MHz superconducting niobium resonators", Phys. Rev. ST Accel. Beams 17, 083501 (2014).
5. L. J. J. Janssen et al., The effect of electrolytically evolved gas bubbles on the thickness of the diffusion layer -II, Electrochimica Acta, **Volume 18**, 543-550 (1973)
6. <https://www.comsol.com/model/flow-in-an-airlift-loop-reactor-10356>